

Real-time simulation and visualization of subject-specific 3D lung dynamics

Anand P Santhanam¹, Cali M Fidopiastis², Paul Davenport³, Katja Langen⁴, Sanford Meeks⁴, Jannick P Rolland^{1,2,5}

¹ School of Computer Science, University of Central Florida

² Institute for Simulation and Training, University of Central Florida

³ Department of Physiological Sciences, University of Florida

⁴ Department of Radiation Oncology, MDAnderson Cancer Center Orlando

⁵ College of Optics and Photonics, University of Central Florida

Abstract

In this paper we discuss a framework for modeling the 3D lung dynamics of normal and diseased human subjects and visualizing them using an Augmented Reality (AR) based environment. The framework is based on the results obtained from pulmonary function tests and lung image-data of human subjects obtained from 4D High-Resolution Computed Tomography (HRCT). The components of the framework include a parameterized pressure-volume (PV) relation estimated from normal human subjects, and a physics and physiology-based 3D deformable lung model extracted from the 4D HRCT data of normal and tumor-influenced human subjects. The parameterized PV relation allows modeling different breathing conditions of a human subject. The 3D deformable lung model allows visualizing the 3D shape changes of the lung for the breathing condition simulated by the PV relation. Additionally, the 3D lung model is deformed using a graphics processing unit (GPU) and its vertex shaders, which satisfies the real-time frame-rate requirements of the AR environment.

1. Introduction

Medical simulation is a critical component for understanding and planning procedural interventions and predicting patient outcomes. The success of medical simulation is evidenced by the fact that over one third of all medical schools in the United States augment their teaching curricula using patient simulators.[1] Medical visualization is a critical component that enables a viewer to better understand a paradigm presented visually. Recent advances in computer technology provide a further revolution in medical visualization that of coupling medical simulations with patient-specific anatomical models and their physically and physiologically realistic organ morphology. Deformation methods can capture the shape change in 3D organ morphology, a key step in modeling of lung dynamics. Current physically based simulation techniques, such as Finite Element Modeling (FEM) and Finite Difference Modeling (FDM), extend the utility of visualizing the complex anatomy and physiology into both 3D space and the fourth dimension of time.[2] Of particular importance is modeling the shape change of high-resolution 3D lung models with a large number of elements (e.g. nodes, triangles). The large number of elements in these high-resolution 3D models contributes to computational complexity of the deformation computation and graphical rendering, therefore limiting the real-time capabilities of the application.

The real-time requirements of the deformation computation may be best understood in the context of a general description of an AR environment employed in 3D visualization as previously described in [3]. The components of this AR environment consist of a Head Worn Display (HWD), an optical tracker, a few landmarks in the physical world, and a virtual scene to be rendered. The landmarks are placed on a physical human patient simulator. The optical tracker tracks the position of the landmarks and the position and orientation of the HWD at the rate of once per 15 msec. A virtual static 3D lung model is superimposed and viewed through the HWD on the human patient simulator. Any changes in the position and orientation of the HWD are tracked and the superimposed virtual lung model is updated and rendered according to the new viewpoint. Fig.1 shows static lungs superimposed over a human patient simulator. To replace this static model with a physiologically correct deformable lung model that is displayed without flicker, the deformation must be computed at greater than one frame per 15 msec. In this paper we discuss a framework that enables visualizing a human subject's specific 3D lung dynamics in an AR environment satisfying real-time frame-rate requirements. The contribution of this paper lies in the integration (reported in section 3.5) of methods previously detailed.

2. Literature review

Lung deformations have been studied for verifying different technologies of medical imaging equipments such as myocardial SPECT, understanding pulmonary mechanics, [4-6] registering MRI images,[7] [8] generating in-vitro lung models,[9] and for medical training purposes [10]. The initial methods to model the 3D human lung deformation were based on physiology and clinical measurements.[11] A significant amount of work has been undergone in understanding and modeling pulmonary mechanics using animal and human data. In these studies, the key parameters extracted from pulmonary imaging modalities are the Green's strain tensor and the Jacobian of the displacement gradient. While the Lagrangian strain tensor provides the change in length of the edges in the 3D data, the Jacobian of the displacement gradient provides insights on the local change in lung volume.

From a simulation and visualization perspective, we concentrate on deforming a given 3D human lung model for a known airflow pattern within the lung. The deformation is modeled by using both the stress and strain components at every lung node and using a physics-based deformation paradigm that relates the stress and strain in a local lung neighborhood. Under this context, the human lung modeling literature has been mainly divided into two approaches: (1) Single compartment model and (2) Multi-compartment model. The physically-based deformation of the human lung model as a linearized single-compartment model was proposed by Promayon.[12] An FEM based single-compartment model was proposed by Decarlo for real-time medical visualization.[13] It was then extended by Kaye in order to model pneumothorax related conditions.[14] Additionally, a visualization-based training method was developed for pneumothorax using a single-compartment model.[10] The method had an analogy for lung deformations to an electrical circuit.[14] A multi-compartment functional FEM model, which modeled the tissue constituents (i.e. parenchyma, bronchiole and alveoli) of lungs was done by Tawhai. This effort aimed in analyzing the anatomical functions of lungs during breathing.[15] The run-time computational complexity of this approach was reduced by modeling solely the bronchioles and the air-flow inside the lung.[16] Of particular importance is the role of airflow inside lungs. Based on medical image analysis, the spatial air distribution inside lungs was shown to be dependent on the gravity and thus the orientation of the subject. From the perspective of a physically-based deformation, the air distribution defines the force applied on the lung model and thus needs to be accounted for. A non-physically based analysis of lung morphology has been extensively investigated in the field of lung physiology and imaging. Some of the key works include the analysis of lung morphology using image warping.[17] A non-physically-based method to lung deformations was also proposed using NURBS surfaces based on imaging data from CT scans of actual patients.[18] The usage of a high-resolution model for lung deformations and its real-time visualization were not addressed in these efforts. From a modeling and simulation perspective, the physically-based deformation methods are suitable for simulating lung dynamics since they allow the inclusion of different breathing parameters.

3. Methods

In this section we discuss an integration of methodologies developed for modeling a pressure-volume (PV) data of a human subject and for modeling real-time 3D lung deformations. It is followed by a discussion on the real-time optimization of the deformation computation using GPU.

3.1 Pressure-Volume relation of human lungs

A method to parameterize the PV relation was discussed by Santhanam et al in [19, 20]. From a modeling and simulation perspective, such an approach allows us to model the PV relations of both normal and disease states (e.g. Chronic Obstructive Pulmonary Disease & Dyspnea). The method takes into account both the control of ventilation and the muscle mechanics. Such an approach allows us to simulate PV curves in different breathing conditions, which can then drive the simulation of 3D lung dynamics for medical visualization applications. The PV relation was represented using both a second-order differential equation that represents the increase and decrease in volume, and a non-linear control function that represents the summary muscle resistance. The control function was given as a linear summation of

products of control parameters and a set of basis functions. The basis functions allowed us to steer the control function, which accounts for variations in the breathing condition. The proposed method can be reversed in order to estimate the values of control parameters from human subject data. Results showed that a set of five control parameters might define accurately the PV relation system. The associated PV relation showed less than 1% RMS difference with the normal human subject data.

3.2 3D deformable lung model

A method to obtain changes in 3D lung shape in a physically and physiologically accurate manner was discussed in [21-23]. As a first step a method to obtain physics and physiology-based deformation method was formulated. Within the context of computer animation, a Green's function (GF) based deformation was chosen since it has been observed that lung deformations do not undergo vibrations. The total number of nodes on each of the 3D high-resolution lung models was approximately 400,000. Such a large number of nodes facilitate effective modeling of both normal and patho-physical lung deformations. Also, a Young's modulus was first associated to every node of the 3D lung model based on the lung's regional alveolar expansion. A unit force was then applied on each node and the transfer function matrix was computed using an iterative approach. In each step of the iteration the force applied on a node was shared with its neighboring nodes based on a local normalization of the Young's modulus coupled with inter-nodal distance. The iteration stopped when this sharing of applied force reached equilibrium. At this point of equilibrium the force shared by a node with its neighbors formed a row of the GF's transfer function matrix.

3.3 Subject specific 3D lung deformations

The physics and physiology-based method was extended in [22] to include human subject based variations in the transfer function. For a known force obtained from the lung physiology and the displacement obtained from a human subject's 4D HRCT data, the changes in the values of the GF's transfer function were computed. Specifically a parameter C was associated with every node that represented the subject specific variations in the transfer function. A spherical harmonics transformation (SHT) of the GF's transfer function row, applied force and the displacement (observed from the subject's 4D HRCT data) was then computed. The parameter C was then computed for each node of the 3D lung model and the GF's transfer function was appropriately modified.

3.4 GPU-based lung deformation

A method to speed-up the computation process of the proposed deformation system was discussed in [24]. A per-vertex approach for deforming and rendering 3D lung models was considered. A method to optimally compute the matrix-vector multiplication in a GPU during run-time was presented. Specifically the matrix-vector multiplication was represented in steps, which can be partially pre-computed off-line. The columns of the transfer function matrix were pre-computed and represented using SHT coefficients. These coefficients were obtained from orthonormal decomposition of the transfer function matrix using SH transformations[25]. This property of SHT allows us to represent the transfer matrix using a minimal number of SH coefficients.

While the 3D models were rendered using a point-based rendering approach, a comparison of the frame rate per second (FPS) in using point-based rendering and polygon-based rendering was discussed. Additionally, the number of SHT coefficients used for representing the transfer function row is very less as compared to the number of coefficients used for shape approximation. The proposed method coupled with the per-vertex nature of the SH coefficients allowed us to use GPU for improving computational-speed.

4 Integration

The sequence of steps involved in obtaining real-time 3D lung dynamics using the methods discussed in sections 3.1, 3.2 and 3.3 is now discussed. The clinical data include four PV curves obtained from normal human subject data, and 4D HRCT data of normal and tumor-influenced human subjects. The PV curves were parameterized using the method discussed in section 3.1. The mean of the control constants associated

with each of the parameterized PV curves was then computed, in order to represent the mean normal PV curves. We then modified the parameterized PV curve to simulate tumor-influenced 3D lungs. We then simulate a change in the motor drive for breathing, caused by the tumor inside the lungs. All three PV curves are as shown in Fig.1. The 3D lung models associated with each of the 4D HRCT datasets were first extracted. The displacement associated with each node of the 3D lung model was computed. The applied force due to the airflow inside the lungs was given by the vertical pressure gradient of the lungs. Using the inverse deformation method discussed in [22] and [23]. We extracted the subject-specific transfer function for the normal and tumor influenced 3D lung models. Using this transfer function we deformed the 3D lung model for a unit increase in volume.

We now discuss the computational speed-up obtained using GPUs. For simulation purposes we consider an Nvidia GeForce4 Go5200 and their CG-based vertex shaders. The 3D lung model at the start of the inhalation together with the estimated transfer function is now considered. The SHT coefficients associated with each row of the transfer function were computed as shown in [26]. The vertex position of each node in the lung model along with the SHT coefficients were transferred into the GPU's vertex array. For a given applied force, the displacement was computed in the vertex shader program executed in the GPU.

The applied force was normalized so that the sum of the applied force magnitude on all the nodes was equal to a unit increase in volume. A unit increase in volume was set as the ratio between the tidal volume of human lungs (i.e. 500 ml) and the product of the deformation steps per second (i.e. 66.66 steps/sec) multiplied by the ventilation rate of inhalation or exhalation (normally 5 sec/breathing).

The simulated 3D lung models at the residual pressure, and 100% tidal pressure of the inhalation cycle are as shown in Fig.2a-b for normal lungs and Fig.3a-b for tumor-influenced lungs. The speed-up obtained using the GPU based computation is as shown in Table.1.

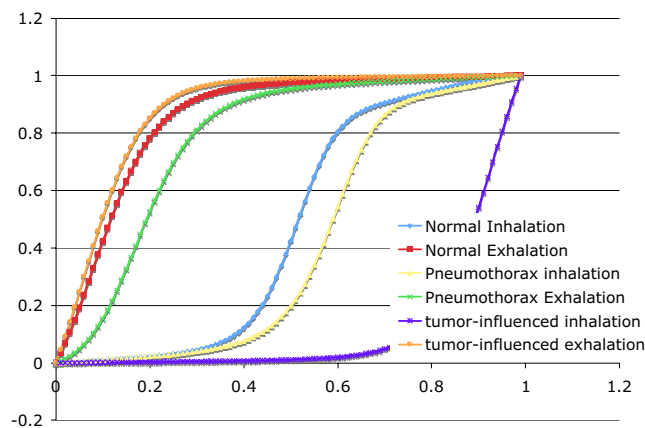


Fig.1. The PV curves generated for normal lung breathing, pneumothorax influenced lung breathing and tumor-influenced lung breathing.

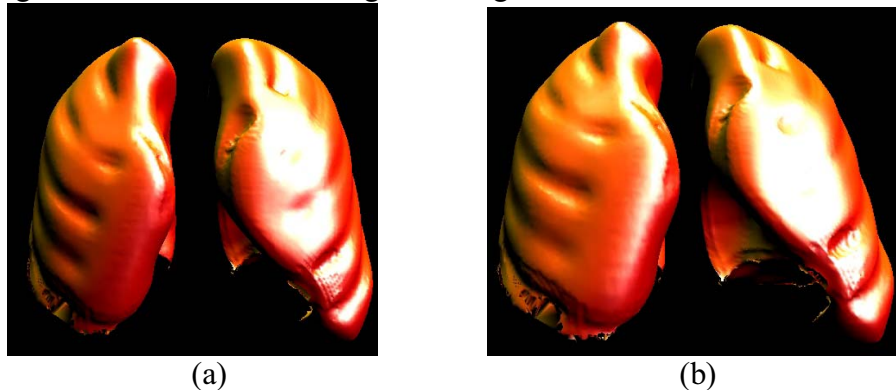


Fig.2. The deformation of a high-resolution lung models obtained from a normal human subject, (a) The lung at residual volume (i.e. before inhalation), (b)The deformed lung at the end of inhalation.

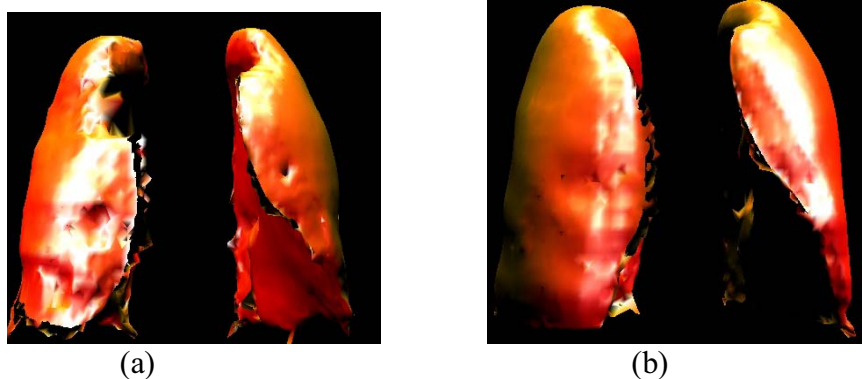


Fig.3. The deformation of a high-resolution lung model obtained from a tumor-influenced human subject, (a) The lung at residual volume (i.e. before inhalation), (b)The deformed lung at the end of inhalation.

Table 1. Frame rates obtained for 3D lung deformations

Approach	FPS- Point-based rendering	FPS - Polygon-based Rendering
GPU based computation	74.46	48.18
CPU based computation	19.90	13.52

5 Discussion

A method to obtain subject-specific 3D lung dynamics is presented in this paper. The method is based on integrating methods discussed in [19, 21, 22, 26]. Such integration may form an effective tool for training clinical technicians on medical procedures,[3] and also for developing guiding systems for treatment procedures such as in radiation oncology[27].

Future work would involve validating the method discussed in this paper and addressing subsequent changes required in each of the methods. Specifically, the transfer function estimated from the subject data is set to remain a constant until the tissue properties undergo irreversible damage. Further validations needs to be done on verifying the constancy of the transfer function. Also the simulated deformation need to be conducted to the verify using invasive analysis of patient-data. Such validations would require a detailed analysis using patient-data with normal and disease conditions, whose results will be discussed in the future.

Reference

1. Good ML, *Patient simulation for training basic and advanced clinical skills*. Medical Education, 2003. 37(s1): p. 14-21.
2. Robb, R.A., *Three-dimensional visualization in medicine and Biology*, in *Handbook of medical Imaging: Processing and Analysis*, I.N. Bankman, Editor. 2000, Academic Press: San Diego,CA.
3. Rolland, J.P., L. Davis, and F. Hamza-Lup, *Development of a training tool for endotracheal intubation: Distributed Augmented Reality*. Medicine Meets Virtual Reality (MMVR), 2003. 11: p. 288-294.
4. Hoffman, E.A., A.V. Clough, G.E. Christensen, C.L. Lin, G. McLennan, J.M. Reinhardt, B.A. Simon, M. Sonka, M. Tawhai, E. Van Beek, and G. Wing, *The comprehensive imaging-based analysis of the lung*. Academy of Radiology, 2004. 11: p. 1370-1380.
5. Gee, J.C., T. Sundaram, I. Hasegawa, H. Uenatsu, and H. Hatabu. *Characterization of regional pulmonary mechanics from serial MRI data*. in *Medical Image Computing and Computer Aided Intervention*. 2002: LNCS.
6. Voorhees, A., J. An, K. Berger, R.M. Goldring, and Q. Chen, *Magnetic resonance imaging-based spirometry for regional assessment of pulmonary function*. Magnetic Resonance in Medicine, 2005. 54: p. 1146-1154.
7. Reinhardt, J.M., R. Uppaluri, W.E. Higgins, and E.A. Hoffman, *Pulmonary imaging and analysis*, in *Handbook of medical imaging*, M. Sonka and J.M. Fitzpatrick, Editors. 2000. p. 1005-1060.

8. Sundaram, T., B.B. Avants, and J.C. Gee. *Towards a dynamic model of pulmonary parenchymal deformation: evaluation of methods for temporal re-parameterization of lung data.* in *Medical Image Computing and Computer Aided Intervention*. 2005: Lecture notes on Computer Science.
9. Guerrero, R.R., D.E. Rounds, and J. Booher, *An improved organ culture method for adult mammalian lung.* *In Vitro*, 1977. **13**(8): p. 517-524.
10. Dawson, S., *A critical approach to medical simulation.* *Bulletin of the American College of Surgeons*, 2002. **87**(11): p. 12-18.
11. Ligas, J.R. and F.P.J. Primiano, *Respiratory mechanics*, in *Encyclopedia of Medical Instrumentation*, J.G. Webster, Editor. 1988, John Wiley & Sons: New York. p. 2550-2573.
12. Promayon, E., P. Baconnier, and C. Puech, *Physically-based model for simulating the human trunk respiration movements.* *Proceedings of International Joint Conference in CVRMed and MRCAS.*, 1997. **1205**: p. 121-129.
13. Decarlo, D., J. Kaye, D. Metaxas, and J.R. Clarke. *Integrating Anatomy and Physiology for behavior modeling.* in *MMVR*. 1995.
14. Kaye, J.M., F.P.J. Primiano, and D.N. Metaxas, *A Three-dimensional virtual environment for modeling mechanical cardiopulmonary interactions.* *Medical Image Analysis*, 1998. **2**(2): p. 169-195.
15. Tawhai, M.H. and K.S. Burrowes, *Developing integrative computational models.* *Anatomical Record*, 2003. **275B**: p. 207-218.
16. Ding, H., Y. Jiang, M. Furmanczyk, A. Prkewas, and J.M. Reinhardt. *Simulation of human lung respiration using 3-D CFD with Macro Air Sac System.* in *Western Simulation Conference Society for Modeling and Simulation International*. 2005. New Orleans.
17. Krishnan, S., K.C. Beck, J.M. Reinhardt, K.A. Carlson, B.A. Simon, R.K. Albert, and E.A. Hoffman, *Regional lung ventilation from volumetric CT scans using image warping functions.* 2004.
18. Segars, W.P., D.S. Lalush, and B.M.W. Tsui, *Modeling respiratory mechanics in the MCAT and the spline-based MCAT systems.* *IEEE Transactions on Nuclear Science*, 2001. **48**(1): p. 89-97.
19. Santhanam, A., C. Fidopiastis, J.P. Rolland, and P. Davenport, *A bio-mathematical formulation for modeling the pressure-volume relationship of lungs (submitted).* *Journal of Applied Physiology*, 2004.
20. Santhanam, A., C. Fidopiastis, and J.P. Rolland. *An adaptive driver and real-time deformation algorithm for visualization of high-density lung models.* in *Medical Meets Virtual Reality 12*. 2004. Newport, CA: IOS Press.
21. Santhanam, A., C. Fidopiastis, F. Hamza-Lup, J.P. Rolland, and C. Imielinska. *Physically-based deformation of high-resolution 3D lung models for augmented Reality based medical visualization.* in *Medical Image Computing and Computer Aided Intervention, AMI-ARCS*. 2004. Rennes, St-Malo: Lecture Notes on Computer Science.
22. Santhanam, A. and J.P. Rolland. *An Inverse deformation method for the visualization of 3D lung dynamics (Abstract).* in *Fourth International conference on Ultrasonic Imaging and tissue elasticity*. 2005. Austin TX.
23. Santhanam, A., C. Fidopiastis, K. Langen, P. Kupelian, S. Meeks, L. Davis, and J.P. Rolland. *Visualization of Tumor-influenced 3D lung dynamics.* in *SPIE Medical Imaging*. 2006.
24. Santhanam, A., C. Fidopiastis, and J.P. Rolland, *3D lung dynamics using a programmable graphics hardware (submitted).* *IEEE Transactions on Information Technology and Biomedicine*, 2005.
25. MacRobert and T. Murray, *Spherical harmonics an elementary treatise on harmonic functions with applications.* International series of monographs in pure and applied mathematics. 1967, New York: Oxford Pergamon Press.
26. Santhanam, A. and J.P. Rolland, *Simulation of 3D lung dynamics using programmable graphics hardware (in review).* *IEEE Information Technology and Biomedicine*, 2006.
27. Murphy, M., *Tracking moving organs in real-time.* *Seminars in Radiation Oncology*, 2004: p. 91-101.